Synthesis of Porous CrO_x Pillared Octahedral Layered Manganese Oxide Materials

Ying Ma[†] and Steven L. Suib*[,†,‡]

Department of Chemistry, U-60, and Department of Chemical Engineering and Institute of Materials Sciences, The University of Connecticut, Storrs, Connecticut 06269

Thorsten Ressler and Joe Wong

Lawrence Livermore National Laboratory, University of California, P.O. Box 808, L-369, Livermore, California 94551

Mark Lovallo and Michael Tsapatsis

Chemical Engineering Department, University of Massachusetts Amherst, 159 Goessmann Laboratory, Amherst, Massachusetts 01003-3110

Received May 25, 1999. Revised Manuscript Received October 6, 1999

Chromium oxide pillared manganese oxide materials were prepared by intercalating layered manganese oxide with chromium hydroxyl acetate clusters under reflux condition. The as-synthesized materials were heated at 200 °C in flowing nitrogen for 1 h to result in chromium oxide pillared manganese oxides. X-ray diffraction, UV−vis, FTIR, BET surface area and pore size distribution, temperature programmed desorption, elemental analysis, and X-ray absorption spectrometry were used to study the intercalating process and the structures of the pillared materials. Porous materials with a high specific surface area and a narrow pore size distribution (18 Å) were obtained. The removal of bound water and dehydroxylated water was responsible for the production of high surface area in the pillared material. The decomposition of acetate groups bidentate-linked to Cr starting at 200 °C in N_2 resulted in a concomitant decrease in porosity. Although the ordering of the layers was largely destroyed and the materials remained "amorphous" under XRD study, TEM morphology studies suggest that the material was still layered. EXAFS studies indicate the formation of Cr−O−Mn bonds in the resultant materials via corner-shared linkages of CrO_6 and MnO_6 octahedra.

I. Introduction

More than two decades has passed since the discovery of robust metal oxide pillared clays in 1977.[1−3] Methods have been developed to prepare pillared materials, which among others, include directly intercalating large Keggin ions, or metal oxohydroxyl oligomers in ready-to-expand clays,[3−8] hydrolyzing metal ions in the presence of clays by means of titration,[9] or intercalating small monomer species which undergo self-polymerization between the layers under reflux.[10−14] Oxide pillared materials are obtained after calcination of the as-synthesized materials at high temperatures (200−400 °C).

The synthesis of pillared materials can be directed to obtain various interesting physical and chemical properties, like thermal stability,[3,4,15−17] porosity,[1,2,18] acidity,[18−21] and catalytic properties.[2,8,22−25] Usually robust main-group metal oxides, for example, Al, Ga,

* To whom correspondence should be addressed
[†] Department of Chemistry, U-60.
[‡] Department of Chemical Engineering and Institute of Materials Sciences.

(1) Szostak, R.; Ingram, C. In *Catalysis by Microporous Materials: Studies in Surface Science and Catalysis*; Beyer, H. K., Karge, H. G., Kiricsi, I., Nagy, J. B., Eds.; 1995; Vol. 94, pp 13−38.
(2) Pinnavaia, T. J. *Science* **1983**, *220*, 365−371.
(3) Brindley, G. W.; Semples, R. E. *Clay Miner.* **1977**, *12*, 229−237.
(4) Yamanaka, S.; Brindley, G. W. *Clays Clay Miner.* **1978**, *27*, 119−124.
(5) Lahav, N.; Shani, U.; Shabtai, J. *Clays Clay Miner.* **1978**, *26*, 107−115.
(6) Brindley, G. W.; Yamanaka, S. *Am. Miner.* **1979**, *64*, 830−835.
(7) Oades, J. M. *Clays Clay Miner.* **1984**, *32*, 49−57.
(8) Pinnavaia, T. J.; Tzou, M.-S.; Landau, S. D. *J. Am. Chem. Soc.* **1985**, *107*, 4783−4785.
(9) Yamanaka, S.; Brindley, G. W. *Clays Clay Miner.* **1978**, *26*, 21−24.
(10) Maclachlan, D. J.; Bibby, D. M. *J. Chem. Soc., Dalton Trans.* **1989**, 895−899.
(11) Maireles-Torres, P.; Olivera-Pastor, P.; Rodriguez-Castellon, E.; Jimenez-Lopez, A.; Tomlinson, A. G. *J. Mater. Chem.* **1991**, *1* (5), 739−746.
(12) Maireles-Torres, P.; Olivera-Pastor, P.; Rodriguez-Castellon, E.; Jimenez-Lopez, A. *J. Sol. State Chem.* **1991**, *94*, 368−380.
(13) Olivera-Pastor, P.; Maireles-Torres, P.; Rodriguez-Castellon, E.; Jimenez-Lopez, A.; Cassagneau, T.; Jones, D. J.; Roziere, J. *Chem. Mater.* **1996**, *8*, 1758−1769.
(14) Yan, Q.; Hou, W.; Chen, Y. *J. Chem. Soc., Chem. Commun.* **1995**, 1865−1866.
(15) Brandt, K. B.; Kydd, R. A. *Chem. Mater.* **1997**, *9*, 567−572.
(16) Kodama, H.; Singh, S. S. *Solid State Ionics* **1989**, 363−372.
(17) Gonzalez, F.; Pesquera, C.; Blanco, C.; Benito, I.; Mendioroz, S. *Inorg. Chem.* **1992**, *31*, 727−731.
(18) Johnson, J. W.; Brody, J. F.; Soled, S. L.; Gates, W. E.; Robbins, J. L.; Marucchi-Soos, E. *J. Mol. Catal. A: Chem.* **1996**, *107*, 67−73.
(19) Bradley, S. M.; Kydd, R. A. *J. Catal.* **1993**, *141*, 239−249.
(20) Shabtai, J. U.S. Patent 4,238,624, 1980.
(21) Shabtai, J.; Lazar, R.; Oblad, A. G. *Stud. Surf. Sci. Catal.* **1981**, *1*, 828−840.
(22) Chen, J. P.; Yang, R. T. *Chem. Eng. Commun.* **1996**, *152−153*, 161−171.

10.1021/cm990326a CCC: $18.00
Published on Web 11/12/1999

Zr, and Si oxides, or their mixtures are used for the purpose of increasing thermal stability,[3,4,17,26] while transition metal oxides, due to their variable valence states, are potential catalysts for many redox organic reactions.[1]

A great deal of research on synthesizing pillaring materials has been focused on using clays as matrixes.[2] More recent research shows that some other layered materials, for example, phosphates,[10−13,27,28] titanates,[26,29] titanoniobates,[14] and hydrous manganese oxides[30] have also attracted attention and are under investigation for intercalating robust metal oxides or catalytically active metal oxides as pillars. These layered materials, unlike clays, are not readily swelled or intercalated. The gallery spaces of this class of layered materials are opened up by treating the layered compound with acid first and then reacting with amines.[27,30] Upon this treatment, the layered compounds are ready to intercalate large pillaring species.

Transition metal oxide pillars such as Fe_2O_3, Cr_2O_3, and V_2O_5 are of interest because they are catalytically active in dehydrogenation, hydrocracking, isomerization, and disproportionation reactions.[23,31−36] Among these, Cr_2O_3 is the one that has been extensively studied because Cr^{3+} is among the very few transition metal ions that self-polymerize under reflux to form polynuclear clusters between the layers.[10−14] Dimers, trimers, and tetramers have been confirmed and exist in aqueous solution in equilibrium,[37−40] and their relative amounts are related to the pH of the solution.[37−40] Methods were developed to prepare Cr oxide pillared materials. The first one involves using $Cr(OAc)_3$ as pillaring reagents under reflux conditions,[10−14,41] another is formed by titrating $Cr(NO_3)_3$ solution with OH^- in the presence of the layered compound,[8,42] while the most commonly used method involves preparing Cr polynuclear pillaring solutions at an OH^-/Cr^{3+} molar ratio no larger than 2.5 first, and then intercalating the Cr species in layered materials.[6,43,44]

Table 1. Sample Nomenclature and Interlayer *d* Spacings of the Resultant Materials vs Reaction Time[a]

sample	concd Cr trimer solution (M)[b]	Cr/Mn mol ratio in batch	12 h (Å)	1 d (Å)	2 d (Å)	4 d (Å)
Cr01	0.008	0.17	18.4	17.0	16.5	16.2
Cr02	0.008	0.44	22.9	21.9	21.0	20.2
Cr03	0.017	0.88	*c*	*c*	25.5[d]	30.6[d]
Cr04	0.017	0.44	15.7	18.2	19.3	20.1
Cr05	0.008	0.88	41.2	40.1	39.1	39.1
Cr06	0.004	0.18	17.2	17.2	17.1	17.1

[a] All of the reactions were done under reflux conditions. [b] The concentration of Cr trimer is expressed as molarity of $Cr_3(OAc)_7(OH)_2$. [c] Broad peak. [d] Shoulder.

As a natural layered manganese oxide, birnessite has the potential to intercalate large species and to form pillared material.[1,45] Although Al_{13} has been successfully intercalated in OL-1 (synthetic birnessite),[30] intercalating transition metal oxides between manganese oxide layers remains a challenge because redox reactions might occur between manganese oxide and the transition metal oxide during the intercalating process. The charge density of the birnessite layers also does not seem to favor intercalation. Questions arise as to whether OL-1 can be pillared by Cr_2O_3 at all, if the layer structure can be kept intact or be destroyed upon intercalation, what the local structure of this material is, and whether a high specific surface area results from this process. This research was designed to try to answer some of these questions.

II. Experimental Section

A. Synthesis of Cr Oxide Pillared OL-1. Preparation of precursors (OL-1) was done as follows: 100 mL of an aqueous solution of 1.58 g of $KMnO_4$ and 12 g of NaOH was added dropwise to 100 mL of an aqueous solution of 5.46 g of $MnCl_2 \cdot 4H_2O$ and 2.03 g of $MgCl_2 \cdot 4H_2O$ with vigorous stirring. The reaction mixture was allowed to stir for another 30 min upon completion of the addition, before the mixture was aged in an 80 °C oven for 2 days. The resultant gray solid was completely washed until the pH of the wash water was around 9. This solid is Na−OL-1, which is characterized by two diagnostic XRD peaks (7.0 and 3.5 Å).

The Na−OL-1 was reacted with 500 mL of 1 M HNO_3 for 24 h, after which the solid was washed completely with distilled deionized water (DDW). The resultant material was H−OL-1, as characterized by two XRD diffraction peaks, 7.3 and 3.65 Å. H−OL-1 was reacted with hexylamine at room temperature for 24 h. The mole ratio of hexylamine to Mn was 5:1. The resultant material was characterized by a set of sharp and high-intensity (00*l*) reflection peaks in its XRD patterns up to the fifth order. This hexylammonium ion pillared OL-1 (HAOL) was the direct precursor for the pillaring process.

$Cr_3(OAc)_7(OH)_2$ aqueous solutions with concentrations of 0.004, 0.008, and 0.017 M were added to HAOL at a molar ratio of Cr to Mn of 0.18, 0.44, and 0.88. The reactions were carried out under reflux for 4 days. The preparation conditions are listed in Table 1. The as-synthesized samples were completely washed with distilled deionized water, dried in air

(23) Choudary, B. M.; Durgaprasad, A.; Valli, V. L. K. *Tetrahedron Lett.* **1990**, *31*, 5785−5788.
(24) Kiricsi, I.; Molnar, A.; Palinko, I.; Fudala, A.; Nagy, J. B. *Solid State Ionics* **1997**, *101−103*, 793−797.
(25) Mitchell, I. V. *Pillared Layered Structures: Current Trends and Applications*; Elsevier: London, 1990.
(26) Hou, W.; Yan, Q.; Chen, Y.; Fu, X. *Preparation of Catalysts VI Scientific Bases for the Preparation of Heterogeneous Catalysts*; Poncelet, G. et al., Eds.; Elsevier Science: New York, 1995; pp 799−805.
(27) Clearfield, A.; Roberts, B. D. *Inorg. Chem.* **1988**, *27*, 3237−3240.
(28) Perez-Reina, F. J.; Olivera-Pastor, P.; Rodriguez-Castellon, E.; Jimenez-Lopez, A. *J. Solid State Chem.* **1996**, *122*, 231−238.
(29) Cheng, S.; Wang, T.-C. *Inorg. Chem.* **1989**, *28*, 1283−1289.
(30) Wong, S.-T.; Cheng, S. *Inorg. Chem.* **1992**, *31*, 1165−1172.
(31) Korby, M. C.; Vaughan, D. W. U.S. Patent 5,364,980, 1994.
(32) Choudary, B. M.; Valli, V. L. K.; Prasad, A. D. *J. Chem. Soc., Chem. Commun.* **1990**, 721−722.
(33) Choudary, B. M.; Valli, V. L. K. *J. Chem. Soc., Chem. Commun.* **1990**, 1115−1116.
(34) Choudary, B. M.; Prasad, A. D.; Bhuma, V.; Swapna V. *J. Org. Chem.* **1992**, *57*, 5841−5844.
(35) Choudary, B. M.; Prasad, A. D.; Swapna, V.; Valli, V. L. K.; Bhuma, V. *Tetrahedron* **1992**, *48*, 953−962.
(36) Lourvanij, K.; Rosser, G. L. *Appld. Catal. A, General* **1994**, *109* (1), 147−165.
(37) Drljaca, A.; Anderson, J. R.; Spiccia, L.; Turney, T. W. *Inorg. Chem.* **1992**, *31*, 4894−4897.
(38) Bradley, S. M.; Lehr, C. R.; Kydd, R. A. *J. Chem. Soc., Dalton Trans.* **1993**, 2415−2420.
(39) Rotzinger, F. P.; Stunzi, H.; Marty, W. *Inorg. Chem.* **1986**, *25*, 489−495.
(40) Stunzi, H.; Rotzinger, F. P.; Marty, W. *Inorg. Chem.* **1984**, *23*, 2160−2164.
(41) Jimenez-Lopez, A.; Maza-Rrodriguez., J.; Olivera-Pastor, P.; Maireles-Torres, P.; Rodriguez-Castellon, E. *Clays Clay Miner.* **1993**, *41* (3), 328−334.
(42) Tzou, M.-S.; Pinnavaia, T. J. *Catal. Today* **1988**, *2*, 243−259.
(43) Volzone, C. *Clays Clay Miner.* **1995**, *43* (3), 377−382.
(44) Sychev, M. V.; Kostoglod, N. Yu.; Astrelin, I. M.; Rozwadowski, M.; Van Oers, E. M. *Kinet. Catal.* **1998**, *39* (1), 106−113.
(45) Ching, S.; Petrovay, D. J.; Jorgensen, M. L.; Suib, S. L. *Inorg. Chem.* **1997**, *36*, 883−890.

at 60 °C, and heated at 200 °C in flowing nitrogen for 1 h to result in CrO_x pillared manganese oxide materials.

B. Characterization. *X-ray Diffraction (XRD) Studies*. A Scintag 2000 PDS diffractometer with Cu Kα radiation (1.54060 Å) was used. The excitation voltage and current were 45 kV and 40 mA, respectively. Countinuous scan data with a scanning rate 5° 2θ/min were acquired for thin-film samples prepared by dripping a slurry of solid sample on a glass microscope slide, followed by air-drying. Step scan data with a step size of 0.02° 2θ were obtained for finely ground powder.

Elemental Analyses on Both Solid Samples and Mother Liquors. An atomic emission spectrometer (ICP-AES) equipped with inductively coupled plasma with a Perkin-Elmer Model 140 system was employed for elemental analyses. Solid samples were dissolved in dilute $HNO_3-H_2O_2$ solutions for Cr and Mn analyses. Mother liquor solutions for these reactions were also analyzed for the same metal ions to determine the efficiency of the pillaring processes.

Thermogravimetric Analysis (TGA). TGA experiments were performed with a TA instrument Model 2950. The as-synthesized samples were air-dried at 60 °C before TGA experiments. Two TGA runs, one in N_2 and the other in O_2, were conducted on each sample from ambient temperature to 900 °C with a heating rate of 10 °C/min. Residues of the TGA experiments were saved for XRD studies.

Temperature programmed Desorption (TPD). A 60 °C air-dried as-synthesized sample (Cr05) was heated in flowing N_2 from ambient temperature to 450 °C with a heating rate of 10 °C/min. The desorbed species were analyzed with a MKS−UTI PPT quadrupole residual gas analyzer mass spectrometer (MS). The temperature was monitored by an Omega CN 2042 temperature programmed controller.

Transmission Electron Microscopy (TEM). The morphology of the pillared material was studied using transmission electron microscopy performed on a JEOL 3010 microscope operated at 300 kV.

Fourier Transform Infrared (FTIR) Spectra. Diffuse reflectance infrared spectroscopy was done with a Nicolet Magna-IR Model 750. The mid IR range was investigated using a mercury−cadmium−telluride (MCT-B) detector and a KBr beam splitter. Resolution of the instrument is up to 0.125 cm^{-1}.

Ultraviolet−Visible (UV−Vis) Spectra: UV−vis analysis on pure Cr trimer solutions and on mother liquor solutions was done with a Hewlett-Parkard 8452A diode array spectrophotometer. The liquid samples were put into a quartz UV−vis cell with the path length being 0.2 cm.

Specific Surface Area and Pore Size Distribution. The specific surface areas of the pillared samples were measured using BET methods. Five point measurements were taken. Both BET surface areas and pore size distributions were performed on an Omnisorp-100CX analyzer with N_2 as the adsorbate at 77 K.

Extended X-ray Absorption Fine Structure (EXAFS) and X-ray Absorption Near Edge Structure (XANES) Experiments. Experiments were performed on the 31-pole-wiggler beamline 10−2[46] at Stanford Synchrotron Radiation Laboratory (SSRL) with the storage ring operating at an energy of 3.0 GeV and an injection current of ∼100 mA. A Si(220) double-crystal monochromator was used to filter out the higher harmonics in the synchrotron beam by detuning the monochromator to ∼50% of the maximum of the rocking curve. Samples were ground and prepared as a thin powder layer on Kapton tape. About six layers of tape were used to improve sample homogeneity and to obtain an absorption edge jump of less than 1.0 absorption length. EXAFS spectra were recorded at room temperature. An equivalent step size of 0.25 eV/point was used for XANES scans and 1.0 eV/point for EXAFS scans. A manganese or chromium metal standard foil located in front of a reference ion chamber was measured simultaneously with each spectral sample for energy calibration.

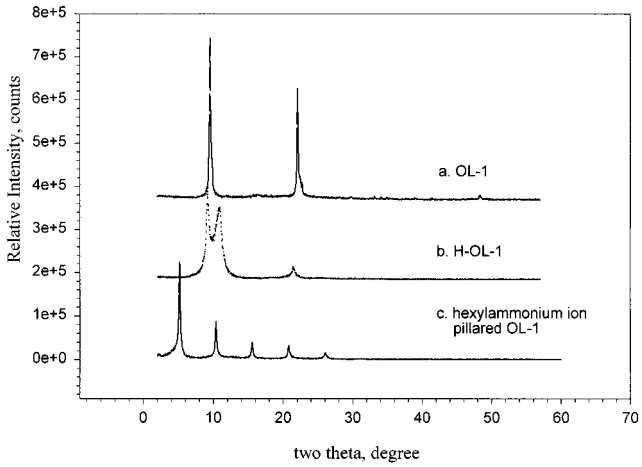

Figure 1. X-ray diffraction patterns of thin film samples: (a) OL-1, (b) H−OL-1, and (c) hexylammonium ion pillared OL-1.

Both EXAFS and XANES data were reduced and analyzed using WinXAS97 v1.1.[47] The energy threshold $E_{0,Ref}$ of the reference metal foil was determined from the first inflection point in the spectrum and raw data were linearly calibrated against the difference between the obtained $E_{0,Exp}$ and the tabulated absorption edge energy for Mn (Mn K edge $E_{0,Ref}$ = 6359 eV).[48] Energy threshold, $E_{0,Exp}$, of each sample spectrum was determined by fitting an arctangent step function to the XANES region. Average Mn valences were then obtained from a calibration curve (Mn valence versus Mn *K*-edge position). Details on the procedure employed can be found elsewhere.[49] A smooth atomic background was calculated using cubic splines. The radial distribution function $FT[\chi(k)]$ was obtained by Fourier transforming the k^3-weighted experimental $\chi(k)$ function multiplied by a Bessel window, into the *R* space.

III. Results

A. The Formation of Cr Cluster Intercalated OL-1. Hexylammonium ion pillared OL-1 (HAOL) was used as a matrix to intercalate Cr species. The matrix was composed of layered manganese oxide with its interlayer space filled by well-ordered hexylammonium ions.[30] The distance between two successive manganese oxide layers is 17.5 Å (Figure 1).

Intercalation reactions between this matrix and the $Cr_3(OAc)_7(OH)_2$ (Cr trimer) were carried out under reflux conditions as described in the Experimental Section. The resultant materials displayed significantly increased interlayer distances as compared to that of OL-1 as shown in Figure 2. The interlayer distances were dependent upon the initial concentrations of Cr trimer solutions and the initial molar ratios of Mn to Cr, as listed in Table 1.

During the course of the intercalation process, samples of the reaction mixtures were periodically collected and X-ray diffraction was performed to monitor interlayer distances. While the dark green color of the Cr trimer solution disappeared in ∼20 min, indicative of the intercalation of Cr species, it took ∼4 days of reflux for the interlayer distances of the samples to reach constant value. Data in Table 1 suggest that during the inter-

(46) Karpenko, V.; Kinney, J. H.; Kulkarni, S.; Neufeld, K.; Poppe, C.; Tirsell, K. G.; Wong, J.; Cerino, J.; Troxel, T.; Yang, J.; Hoyer, E.; Green, M.; Humphries, D.; Marks, S.; Plate, D. *Rev. Sci. Instrum*. **1989**, *60*, 1451−1456.

(47) Ressler, T. *J. Synch. Rad*. **1998**, *5*, 118−122.

(48) Bearden, J. A.; Burr, A. F. *Rev. Mod. Phys.* **1967**, *39*, 125−142.

(49) Ressler, T.; Brock, S. L.; Wong, J.; Suib, S. L. *J. Phys. Chem. B* **1999**, in press.

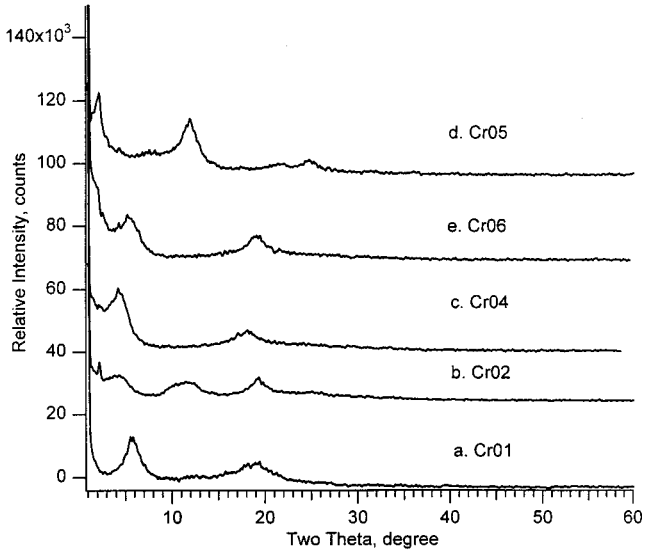

Figure 2. X-ray diffraction patterns of thin film as-synthesized samples: (a) Cr01, (b) Cr02, (c) Cr04, (d) Cr05, and (e) Cr06.

calation process, the intercalated Cr hydroxyl clusters might rearrange in the interlayer space in a concentration dependent manner.

C analysis on the postreflux samples shows that the molar ratios of C to Cr of the intercalated species decreased from 14:3 in the Cr trimer to less than 1:1 in these postreflux samples, in other words, only 5−16% of acetate groups in the Cr trimer were preserved after reflux. This strongly indicates that Cr species had been largely polymerized during reflux−intercalation and hydroxo or oxo ligands might replace the bidentate-linked acetate groups.

B. The Amounts of Cr Loaded in Manganese Oxide Matrixes. Upon completion of the four-day intercalation, about 1% or less of the initial Cr remained in solution for all of the samples with the exception of Cr03, where 4% of the initial Cr was detected. Therefore, the majority of Cr species was intercalated between the manganese oxide layers regardless of the initial concentration of Cr trimer pillaring solution and the initial molar ratio of Cr to Mn.

Two UV−vis peaks, located in the vicinity of 576 and 430 nm, are characteristic of Cr^{3+} ions of six-coordinate geometry and correspond to the two transitions $^4T_{2g} \leftarrow {}^4A_{2g}$ and $^4T_{1g} \leftarrow {}^4A_{2g}$.[40] These transitions move to higher energies when more Cr ions exist in Cr clusters or the molar ratio of OH to Cr decreases (i.e., as condensation and polymerization increase).[38,40] The UV−vis results of the mother liquors (Cr01 to Cr06) showed that no Cr species were present with the sole exception of Cr03, which exhibited weak and broad peaks at 407 and 558 nm (Figure 3). The large blue shifts of these two peaks from 430 and 576 nm of the Cr trimer suggest that Cr species larger than the Cr trimers were formed in solution which might be too large to be intercalated.

Elemental analyses were also conducted on the resultant postreflux solid samples (Table 2). These samples (hereafter referred to as, *as-synthesized* samples) were extensively rinsed with distilled deionized water to remove physi-adsorbed Cr species prior to analyses before the elemental analysis was conducted. Partially due to the dissolution of Mn^{2+} into mother liquor from

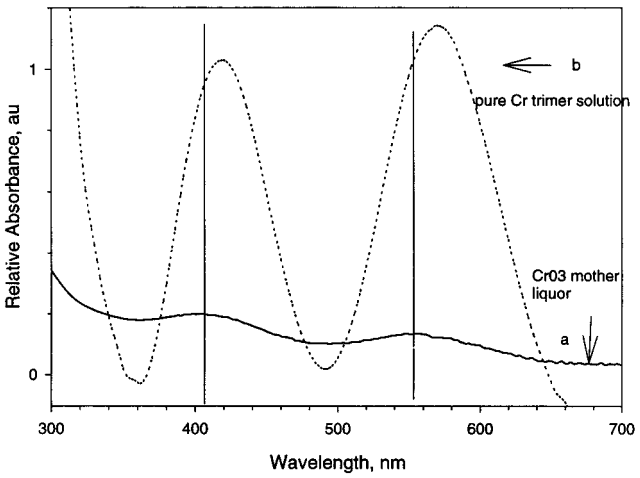

Figure 3. UV−vis spectra of mother solutions of Cr03 (a) showing blue shifts of the two characteristic UV−vis peaks as compared to pure Cr trimer solution (b) from which Cr03 was prepared.

Table 2. Elemental Analyses of the Intercalated Samples and BET Results Using N_2 as Adsorbate (m^2/G)[a]

sample	mol ratio Cr/Mn	*T*, °C 150	200	250	400
Cr01	0.17	93	162		119
Cr02	0.45		248		
Cr03	0.97		269	247	
Cr04	0.46		220		
Cr05	1.23		283	251	
Cr06	0.18	88	171		117

[a] The heat treatment was conducted in nitrogen atmosphere unless otherwise stated. BET results for OL-1 and hexylammonium ion pillared OL-1 are 41 and 46 m^2/g, respectively, and 83 and 89 for Cr03 and Cr05 heated at 200 °C in O_2 for 1 h, respectively.

the OL-1 framework, the molar ratios of Cr to Mn in the solid samples spanned a large range from 0.17 to 1.23 in our six samples. The largest difference between batch and the resultant material was found in Cr05, where the dissolution of Mn^{2+} was the most severe. These data indicate that by varying the Cr/Mn molar ratio and the concentration of Cr trimers in solution that pillared samples with different amounts of intercalated Cr cluster can be created.

C. Specific Surface Area and Pore Size Distribution. The as-synthesized intercalated OL-1 samples did not exhibit greater BET surface areas when compared to the OL-1 sample (51 m^2/g for as-synthesized Cr05 vs 41 m^2/g for the unintercalated OL-1 precursor). However, the BET surface areas of these as-synthesized samples were greatly increased after being heated in flowing N_2 for 1 h (Table 2), whereas heating in air only slightly increased their BET surface areas (Table 2).

A series of heat treatments was conducted in flowing N_2 at 150 °C, 200 °C, 250 °C, and 400 °C, respectively, for 1 h. As shown in Table 2, the optimal temperature for production of largest porosity in the resultant materials was 200 °C. Raising the temperature to 250 °C and 400 °C resulted in ~10% and 30% decrease, respectively, in BET surface areas. Using a temperature of 150 °C was not adequate for the removal of water or organics bound or stuffed in the intercalated materials.

As indicated in Table 2, as the Cr/Mn molar ratio in the intercalated OL-1 increased, so did the BET surface

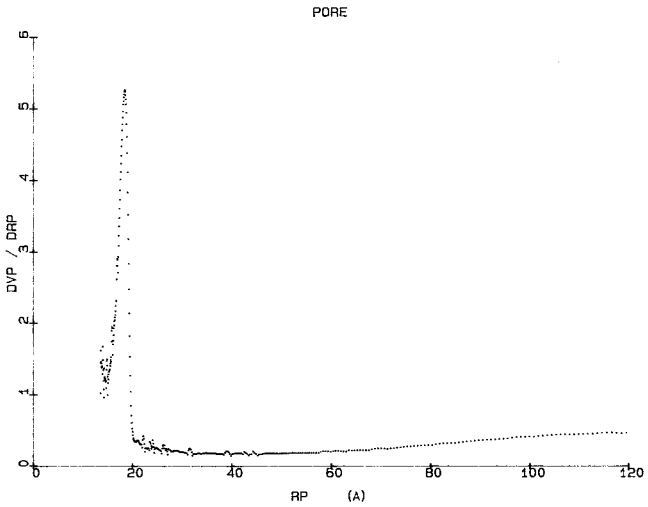

Figure 4. Pore size distribution of Cr05 heated at 200 °C in N_2 for 1 h.

area. This suggests that the intercalation of more Cr species into the OL-1 matrix did not stuff the interlayer space but instead increased the porosity of these materials.

Pore size distribution measurements were conducted on the 200 °C/N_2 heat-treated Cr05 sample that showed the largest BET surface area. This sample exhibited a narrow pore size distribution with the pore diameters of about 18 Å (Figure 4) based on a cylindrical pore model. The TEM morphology of the same heated sample exhibits a layered structure with an interlayer distance of ~26−30 Å (Figure 5), decreased from ~39 Å of the as-synthesized Cr05. None of the heated samples showed XRD patterns, in agreement with previous reports on similar transition metal oxide pillared materials.[10,28,37]

D. The Effects of Heating Atmosphere and Temperature on Porosity. The as-synthesized samples were dried in a 60 °C oven for 3−4 days before TGA, TPD, and in-situ FTIR experiments, where most of the bound or physisorbed water evolved. All samples (Cr01 to Cr06) showed similar weight loss patterns within the same atmosphere. TGA results for sample Cr05 are plotted in Figure 6. Below 250 °C, the rate of weight loss and relative weight loss were greater in O_2 than in N_2, suggesting that different processes occur during heating in different atmospheres.

Temperature-programmed desorption (TPD) was conducted on air-dried Cr05 to identify the species evolved during heating in N_2 (Figure 7). The species evolved below 200 °C were H_2O, ascribed mainly to the dehydroxylation of the polynuclear Cr hydroxo species. The peaks of CO_2 and CH_4, attributable to the decomposition of acetate groups, appeared at about 200 °C and were maximized at about 270 °C. Tails of these two peaks did not diminish until above 400 °C. The peak of water was maximized at the same temperature as that for CO_2 and CH_4, indicating that water released at this temperature may also come from the acetate groups.

In situ FTIR was also conducted on sample Cr05 to study the decomposition or combustion of acetate groups during heating. Two IR peaks, located at 1561 and 1447 cm^{-1}, are characteristic of asymmetric and symmetric vibrations of OCO bonds in acetate groups via bidentate linkages to the metal ions.[50,51] In O_2, the two peaks started to decrease in intensity at 150 °C and disappeared at 250 °C (Figure 8A). In contrast, the intensity of these two peaks did not decrease in N_2 until above 200 °C, and were still present after 300 °C (Figure 8B).

From BET results, the largest porosity of the intercalated materials was obtained with a heat treatment at 200 °C in flowing N_2. With the decomposition of acetate groups above 200 °C in N_2, the BET surface areas decreased. Therefore, removal of bound and dehydroxylated H_2O while preserving acetate groups are important in developing porous structures in chromium oxide intercalated OL-1.

E. XANES and EXAFS Results. XANES measurements were conducted on sample Cr05 to determine the valences of Mn and Cr during intercalation.[48,49,52] The detailed information about data collection and data processing has been described in the Experimental Section. The valences of Mn in our materials were extracted from precalibrated standards as shown in Figure 9R. A slight increase of the valence of Mn was observed from OL-1 (3.31) to HAOL (3.47) followed by a decrease to the as-synthesized Cr05 (3.21), and further to 200 °C/N_2 heated Cr05 (3.18) (Figure 10A).

In Cr K-XANES spectra, both the as-synthesized and heat-treated (200 °C, N_2) Cr05 revealed a low intensity preedge peak at 5989 eV, due to 1s → 3d electron transitions in $Cr^{III}O_6$ octahedra[53,54] as shown in Figure 10B. Cr K-XANES spectra did not support evidence for an enhanced preedge peak characteristic of $Cr^{VI}O_4$ tetrahedra.[13,53−55] This indicated that no significant change of Cr valence state occurred during the pillaring process. The slight valence reduction of Mn during the heating was therefore not likely due to redox reactions between Mn and Cr.

EXAFS measurements were done to determine the local structures of the sample of Cr05. Control experiments with OL-1 and HAOL showed edge-shared linkages characteristic of a layered structure,[54,56,57] as shown in the Mn radial distribution EXAFS spectra in Figure 11A. A new peak at ~3.2 Å developed for the as-synthesized Cr05 and the intensity of this peak further increased upon heating indicative of an increase in the amount of this linkage. In a typical tunnel structured manganese oxide (for example, a 2 × 4 manganese oxide) the distance between Mn and Mn via corner-linked MnO_6 units is ca. 3.1 Å (Figure 11A), and the distance between Cr and Cr via corner-linked CrO_6 is ~3.4 Å (Figure 11B).[53,54,58] In our CrO_x intercalated OL-1, this 3.2 Å peak is believed to be due to the

(50) Erre, L. S.; Micera, G.; Glowiak, T.; Kozlowski, H. *J. Chem. Educ.* **1997**, *74* (4), 432−435.
(51) Johnson, M. K.; Powell, D. B.; Cannon, R. D. *Spectrochim. Acta* **1981**, *37A* (11), 995−1006.
(52) Manceau, A. A.; Gorshkov, A. I.; Drits, V. A. *Am. Miner.* **1992**, *77*, 1133−1143.
(53) Jones, D. J.; Roziere., J.; Maireles-Torres, P.; Jimenez-Lopez, A.; Olivera-Pastor, P.; Rodriguez-Castellon, E.; A. G. Tomlinson, A. A. G. *Inorg. Chem.* **1995**, *34*, 4611−4617.
(54) Manceau, A. A.; Charlet, L. *J. Coll. Interface Sci.* **1992**, *148* (2), 425−442.
(55) Kutzler, F. W.; Natoli, C. R.; Misemer, D. K.; Doniach, S.; Hodgson, K. O. *J. Chem. Phys.* **1980**, *73* (7), 2374−2387.
(56) Sivester, E.; Manceau, A.; Drifts, V. A. *Am. Miner.* **1997**, *82*, 962−978.
(57) Manceau, A. A.; Gorshkov, A. I.; Drits, V. A. *Am. Miner.* **1992**, *77*, 1144−1157.
(58) Bornholdt, K.; Corker, J. M.; Evans, J.; Rummey, J. M. *Inorg. Chem.* **1991**, *30* (1), 1−2.

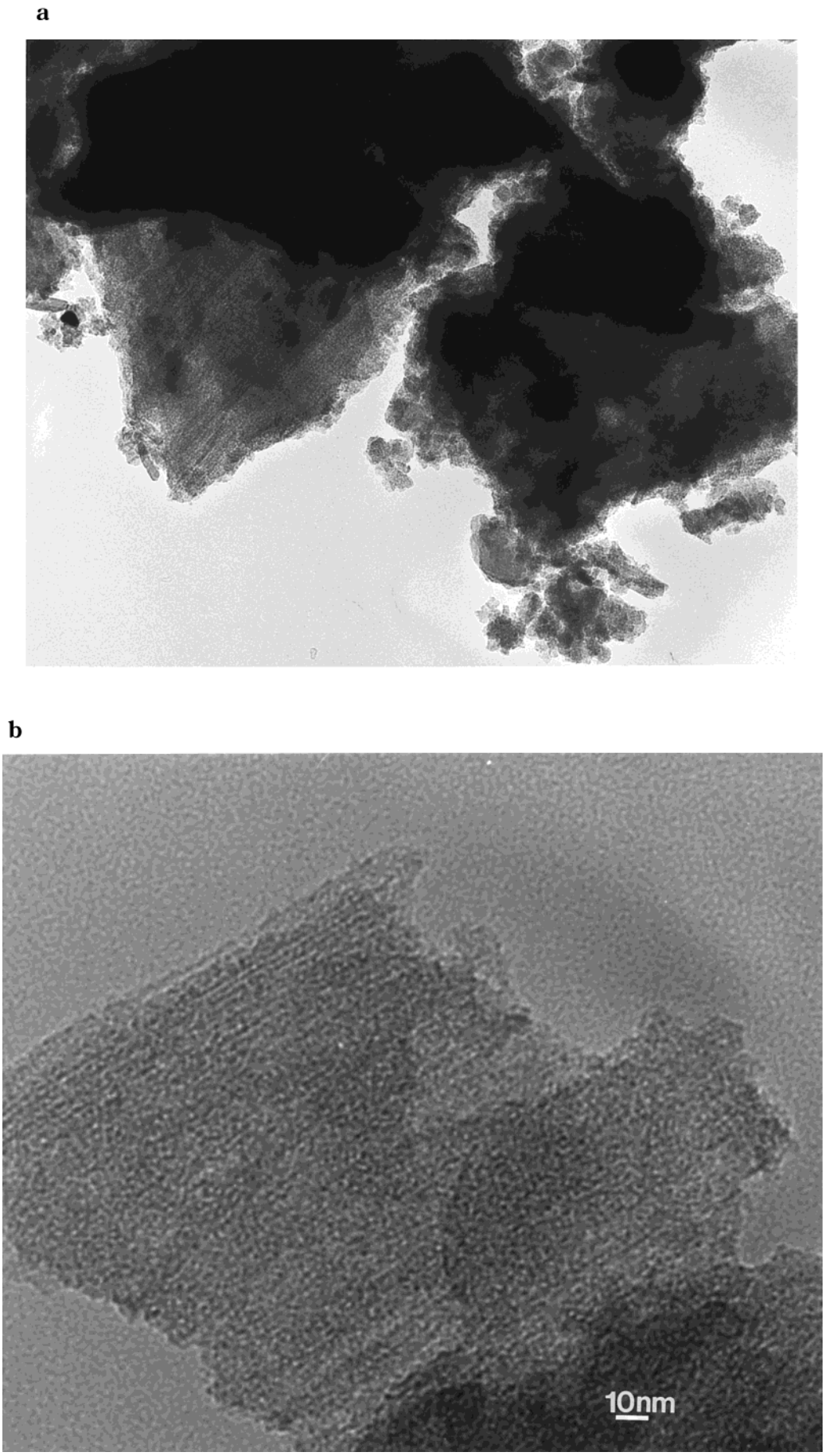

Figure 5. TEM morphology of Cr05 after being heated at 200 °C in N_2 for 1 h. Low magnification image (a) is at 150000×. The higher magnification image (b) (∼1000000×) reveals a disordered layered structure with a predominant spacing of 26−30 Å.

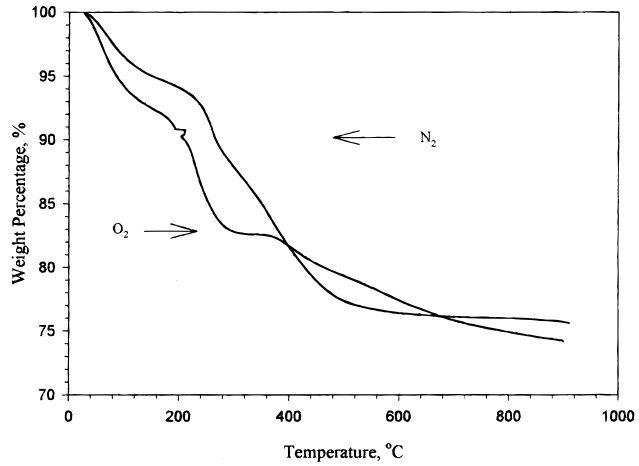

Figure 6. Thermogravimetric analyses (TGA) carried out on sample Cr05 from room temperature to 900 °C with a heating rate of 10 °C/min in both N_2 atmosphere and O_2 atmosphere.

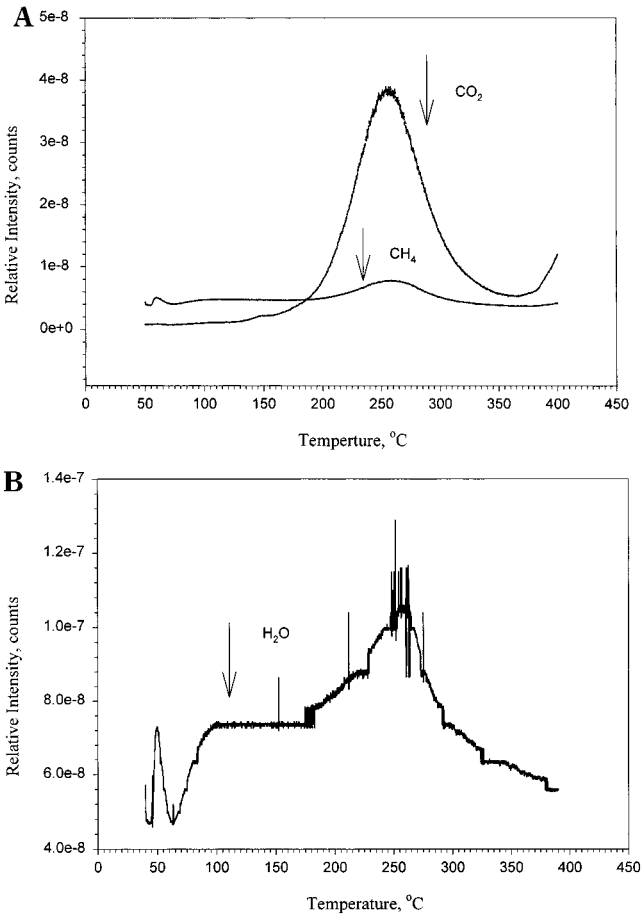

Figure 7. Temperature programmed desorption (TPD) conducted on Sample Cr05 in flowing nitrogen from 60 °C to 450 °C with a heating rate of 10 °C/min: (A) the evolution of CO_2 and CH_4 and (B) the evolution of H_2O.

formation of corner-linked MnO_6 and CrO_6, suggesting the formation of Cr−O−Mn bonds in the intercalated materials.

The Cr EXAFS spectra of the as-synthesized Cr05 and 200 °C heated Cr05 samples were very different from that of the chromium trimer, as shown in Figure 11B. These Cr cluster intercalated materials showed similar spectra to that of Cr_2O_3 (Figure 11B). The first three Cr EXAFS peaks of the intercalated samples exhibit

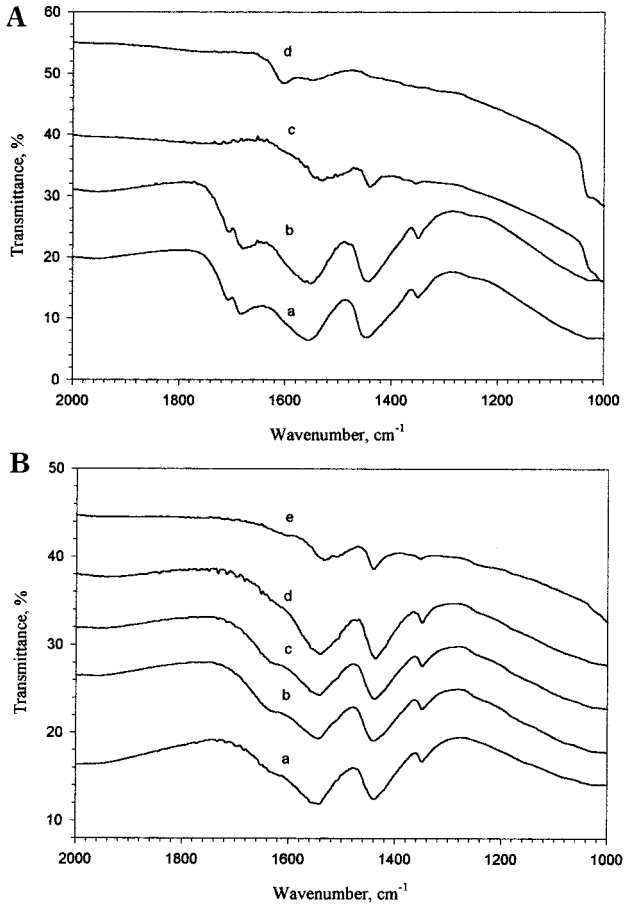

Figure 8. In situ FTIR spectra of sample Cr05 showing the decomposition or combustion of acetate groups: (A) in O_2 atmosphere; (B) in N_2 atmosphere (a, room temperature; b, 100 °C; c, 200 °C; d, 250 °C; e, 300 °C).

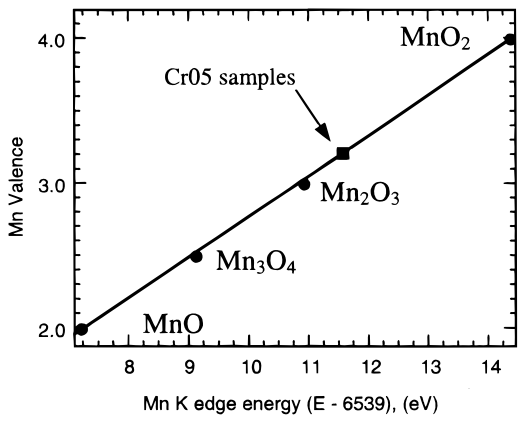

Figure 9. Mn valence vs experimental Mn K-edge position for model manganese oxide compounds. The solid square indicates the edge positions of the Cr05 sample.

similar positions (1.98, 3.06, and 3.40 Å) and amplitudes as those of Cr_2O_3,[53,54] whereas longer distances in our intercalated samples were quickly dampened due to less long range ordering or the reduced size of CrO_x pillars.[53] These three peaks correspond to the bonds of Cr−O in CrO_6 octahedra, Cr−Cr through edge shared CrO_6 octadedra, and Cr−Cr through corner-shared CrO_6 octahedra, respectively. The 2.95 Å Cr FT EXAFS peak of the Cr trimer, attributable to the Cr−Cr bond in the trimer, was absent in the intercalated samples. This suggests that during intercalation that the trimer

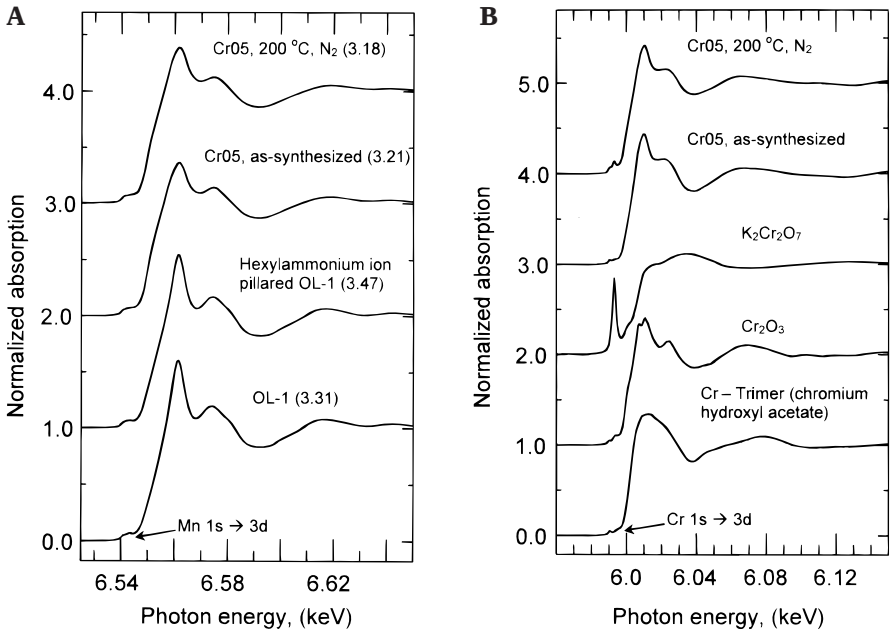

Figure 10. (A) Mn *K*-XANES spectra of OL-1, hexylammonium ion pillared OL-1, as- synthesized Cr05, and Cr05 heated at 200 °C in N_2; and (B) Cr *K*-XANES spectra of Cr trimer, Cr_2O_3, $K_2Cr_2O_7$, as-synthesized Cr05, and 200 °C N_2 heated Cr05.

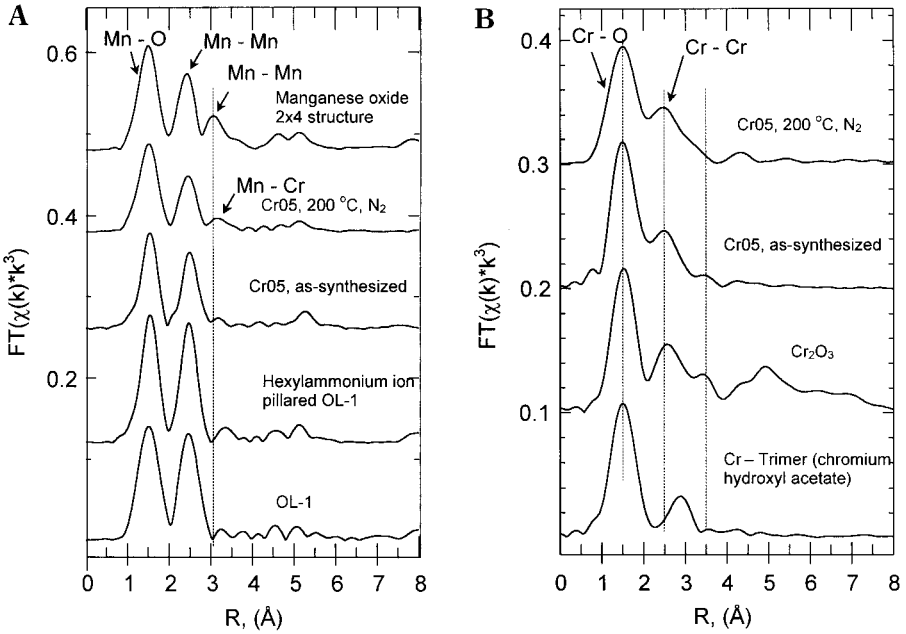

Figure 11. (A) Fourier transformed EXAFS spectra of Mn in OL-1, hexylammonium ion pillared OL-1, as-synthesized Cr05, Cr05 heated at 200 °C in N_2, and Mn oxide 2 × 4 structure (as a reference); and (B) Fourier transformed EXAFS spectra of Cr in Cr trimer (chromium hydroxyl acetate), Cr_2O_3, as-synthesized Cr05, and 200 °C N_2 heated Cr05.

undergoes dissociation, rearrangement and polymerization and that Cr hydroxide clusters are formed at the expense of the Cr trimer.

IV. Discussion

A. The Intercalation Process. Chromia has been intercalated into many different layered compounds including clays,[6,8,37,41−44,58] phosphates,[10−13,28] and titanoniobates,[14] by two different approaches. With layered compounds that are easily swelled in water, such as clays, the synthesis involves direct intercalation of large Cr polynuclear species into clay layers,[6,8,42−44,58] that are produced ex situ. However, solution equilibria among various Cr^{3+} species usually lead to both lateral disorder and stuffing of the interlayer space.[12,13] With layered compounds that are hard to swell in water, the general approach is refluxing the mixture of the layered compounds intercalated with organic ammonium ions and $Cr(OAc)_3$ aqueous solutions. Polymerization of Cr species is believed to occur in situ on the interlayer surfaces of the layered compounds and is therefore regarded as a cleaner route to prepare pillared materials.[11−13,41]

On the basis of the above literature results, hexylammonium ion pillared OL-1 (HAOL) were allowed to contact and react with $Cr_3(OAc)_7(OH)_2$ (Cr trimer) solution under reflux conditions. This Cr trimer is commercially available and has a size of ∼5 Å × 6.5 Å,[53] which is smaller than the gallery space of HAOL and is expected to enter the interlayer space.

The intercalation was indeed rapid, as evidenced by the disappearance of the characteristic dark green color of the Cr trimer in ~20 min. About 99% of the Cr in the pillaring solution was intercalated between the manganese oxide layers regardless of the batch Cr/Mn molar ratio and the Cr trimer concentration in pillaring solution. After the intercalation process, all the as-synthesized materials showed expanded interlayer distances (Table 1) indicative of the intercalation of Cr polynuclear species. These materials, however, did not exhibit good crystallinity, different from what was observed with chromia pillared α-phosphates,[11,12] which were also prepared with the reflux method.

Many reasons account for the poor crystallinity of the materials synthesized in this research. First of all, un-intercalated OL-1 is a much less crystalline material than un-intercalated phosphates. Second, unlike phosphates, OL-1 (a manganese oxide material) is very sensitive to the pH of its environment. With acid treatment of OL-1 by 1 M HNO_3, Mn^{3+} ions in the OL-1 layers disproportionate to Mn^{4+} and Mn^{2+}. Some Mn^{2+} ions dissolve into the mother liquor while some readsorb above or below the vacant sites left by Mn^{3+}, accompanied by an increase of AOS of Mn in OL-1 samples, as confirmed by Mn XANES studies (Figure 10A). With the contact and reaction of Cr trimer solution with HAOL under reflux, more Mn^{2+} dissolved back into the mother liquor, accompanied by a local structural change of the manganese oxide layers.[59,60] The dissolution of Mn^{2+} becomes more extensive when the molar ratio of Cr/Mn in the reaction mixture was increased from 0.44 to 0.88, which may bring more damage to the structure of the manganese oxide matrix.

In addition, Mn XANES studies show that the AOS of Mn decreased from 3.47 in HAOL to 3.21 in the as-synthesized Cr05 despite the dissolution of Mn^{2+} into solutions. We believe that this phenomenon is due to oxygen evolution from the OL-1 framework during the 4-day reflux period instead of redox reactions between Cr and Mn, since Cr^{3+} was not significantly oxidized during the reflux−intercalation process (Figure 10B). Last, $Cr_3(OAc)_7(OH)_2$ other than $Cr(OAc)_3$ was used as the intercalating species. The Cr trimer was not intercalated directly into the OL-1 interlayer spaces as expected but underwent dissociation before polymerization (Figure 11B). This additional step (dissociation) of Cr trimer compared to $Cr(OAc)_3$, complicated the intercalation process and affected the formation of Cr polynuclear species and the crystallinity of the Cr cluster intercalated OL-1 materials.

Despite the complexity of the intercalation process, all syntheses conducted in this research indicate almost complete intercalation of Cr^{3+} species which demonstrates the efficiency of the intercalation process. The Cr^{3+} species remaining as a mother liquor in sample Cr03 indicates that as the concentration of the Cr trimer solution increases, the formation of Cr polynuclear species in solution competes with the intercalation of Cr species and eventually an equilibrium was reached between these two processes.[12]

B. The Intercalated Cr^{3+} Species between Manganese Oxide Layers. The intercalation and calcination of Cr^{3+} species between the OL-1 layers led to an increase in porosity, and more interlayer Cr resulted in larger porosity, although no simple relationship between BET surface area and the interlayer distance is not readily drawn from our data. For example, samples Cr02 and Cr04 have the same interlayer distances and similar Cr/Mn molar ratios (Tables 1 and 2). However, their BET surface areas are different by more than 10%. This is evidence that different Cr species were intercalated in these two materials due to different reaction conditions.

X-ray diffraction and UV−vis spectroscopy which are ideal characterization methods to study Cr species in highly crystalline chromia pillared phosphates,[11−13] were not so useful in this study due to poor crystallinity and the mixed valence of our materials. Mn and Cr EXAFS spectra were used to study the local structures with TEM used to study the morphology of the materials. These results show that the intercalated materials are still layered, while Cr−O−Mn bonds are formed via corner-shared linkages of MnO_6 and CrO_6 octahedra, indicating the incorporation of Cr^{3+} species into the OL-1 layers. The intercalated Cr species have structures similar to Cr_2O_3 but the size of the pillars does not permit long-range ordering.

The bidentate-linked acetate groups are largely replaced during reflux with the concomitant polymerization of the intercalated Cr species. The largest porosity was obtained by removing bound and dehydroxylated water, which was done at 200 °C. On the basis of experimental observations, the decomposition of acetate groups (>200 °C), which may cause structural collapse, did not favor the formation of pores in CrO_x pillared OL-1. The heated Cr05 was allowed to contact water for 24 h before being heated again to 200 °C in N_2. The reheated Cr05 completely preserved the porosity with a BET surface area of 281 m^2/g. This strongly indicates that the removal of water was responsible for production of porosity in our materials and the chromia pillars have been grafted to manganese oxide layers.

XRD on TGA residuals shows that reduced manganese oxides were observed while no chromium oxide was detected for any of our samples regardless of TGA atmosphere. This strongly suggests that Cr species are highly dispersed in the intercalated OL-1 materials. This is different from chromia pillared phosphates, where chromium oxide phase separated during heating in O_2. Our data suggest that the bonds between Cr and Mn via O are fairly strong.

No significant redox reactions occurred between manganese oxides and Cr^{3+} species during the intercalating processes in this research, although research conducted by Manceau et al. clearly shows that Cr^{3+} species were oxidized at the surfaces of birnessite (the natural form of OL-1).[54,61] The lack of redox reactions between matrix and pillaring species in our systems might be ascribed to the fast intercalation of Cr^{3+} species into OL-1 matrix and the robustness of the polymeric forms of Cr^{3+} species formed in the interlayer space.

(59) Ruetschi, P.; Giovanoli, R. In *Proc. Intern. Symp. On Manganese Dioxide*; Schumm, B., Jr., Joseph, H. M., Kozawa, S., Eds.; 1980; Vol. 2, pp 552−558.

(60) Drits, V. A.; Silvester, E.; Gorshkov, A. I., Manceau, A. *Am. Miner.* **1997**, *82*, 946−961.

(61) Silvester, E.; Charlet, L.; Manceau, A. *J. Phys. Chem.* **1995**, *99*, 16662−16669.

V. Conclusions

Cr hydroxyl clusters were intercalated into layered manganese oxide materials by reflux methods. Upon heating at 200 °C in N_2, porous CrO_x pillared layered materials were obtained. The pillars (or the intercalated species) were no longer structurally similar to that of Cr hydroxyl acetate, the pillaring agent in this study, but more like Cr_2O_3. These pillared materials were amorphous as determined by XRD experiments due to irregularity and disorder of the layers, while they still retained a layered structure as determined by TEM. Pore size distributions showed a narrow pore size of ~18 Å for sample Cr05. EXAFS results indicate the formation of corner-shared linkages of MnO_6 and CrO_6 after Cr hydroxyl clusters were intercalated into the manganese oxide interlayer space. Heating the Cr hydroxyl cluster intercalated materials in flowing nitrogen at 200 °C is the best way to achieve high porosity in these systems.

Acknowledgment. We thank the U.S. Department of Energy, Office of Basic Energy Science, Division of Chemical Science, for support of this work. We thank Dr. F. S. Galasso for helpful discussions. Y. Ma thanks Mr. Guan-Guang Xia for providing the 2 × 4 manganese oxide. T. Ressler acknowledges the Alexander-von-Humboldt Foundation, Germany, for a Feodor Lynen Research Fellowship. M. Tsapatsis and M. Lovallo acknowledge support from the David and Lucile Packard Foundation through a fellowship in Science and Engineering for M.T.

CM990326A